Recovery and reuse of carbon fibre and acrylic resin from thermoplastic composites used in marine application

Haithem Bel Haj Frej, Romain Léger, Perrin Didier, Patrick Ienny, Pierre Gérard, Jean-François Devaux

Recovery and reuse of carbon fibre and acrylic resin from thermoplastic composites

Haithem Bel Haj Frej[1], Romain Léger[1], Didier Perrin[2*], Patrick Ienny[1], Pierre Gérard[3], Jean-François Devaux[4]

[1] *LMGC, IMT Mines Ales, Univ Montpellier, CNRS, Ales, France*

[2] *Polymers Composites and Hybrids (PCH), IMT Mines Ales, Ales, France*

[3] *Arkema France, Groupement de Recherches de Lacq, 64170 Lacq, France*

[4] *Arkema France, CRRA, rue Henri Moissan, 69491 Pierre Bénite, France*

*corresponding author: didier.perrin@mines-ales.fr

Abstract

The development of new sustainable routes towards better environmental footprint of composites for marine boatbuilding is motivated by the absence of eco-friendly and economically viable recycling techniques to deal with growing end-of-life thermoset boats waste and increasing restrictive legislation. Thermoplastic composites may offer the possibility to recover raw materials from retired parts, which could have a substantial environmental and economic benefit. This study investigates the feasibility of recovery and reuse of both reinforcement and matrix from a carbon fibre reinforced thermoplastic Elium composite. An original pyrolysis process allowed the depolymerisation of the acrylic matrix and recovery of clean carbon fibres and matrix monomer. Distillation was used to purify the monomer from impurities and a recycled Elium resin was synthesized and reused as matrix with long and aligned recycled carbon fibre reinforcement. The study of the morphological and composition differences at fibre scale resulted in concluding that sizing has been decomposed during depolymerisation process and only small traces of polymer were left on fibre surface. Virgin and recycled resin reinforced with carbon fibre laminates were produced by resin infusion. While tensile modulus, strength and strain at break were nearly unchanged, interlaminar shear strength results showed enhanced fibre-matrix interphase bonding. Dynamic mechanical analysis confirmed the good quality of recovered carbon fibres as well as similar virgin and re-polymerised resin properties. The new composite made from both recycled fibre and matrix could be used in the same application field.

Keywords

Recycling; carbon fibre; thermoplastic composite; mechanical properties; Formulated plastics; marine application

1. Introduction

Fibre reinforced thermosets and thermoplastic resins are increasingly used to replace conventional materials in a number of construction, transport, renewable energies and sporting applications. The increasing demand on Fibre Reinforced Polymers (FRP) is explained by numerous advantages such the high strength to weight ratio, corrosion resistance and enhanced stiffness. The worldwide composite market is growing and it is especially the case of Carbon Fibre Reinforced Plastics (CFRP) market segment. The CFRP global demand has reached 129 kt in 2018 and was estimated to reach 142 kt in 2019, which represents around 10% growth (Sauer, 2019). In Europe, the Glass Fibre Reinforced Plastics (GFRP) production volume trend for 2019 is forecasted to remain stable at 1141 kt, after 10 years of moderate growth. In a recent market review, the glass fibres are used as a reinforcement in over 87% of the total volume of produced composites, compared to just 1.3% for carbon fibres (Witten and Mathes, 2019). In the following paragraph, an overview of marine composite history and market growth will be presented. Further, a brief introduction to the boat's end-of-life issues and techniques of composite recycling will be discussed.

1.1. Case of composites in the marine environment: history, market growth and end-of-life issues

In marine industry sector, especially boatbuilding, a similar increasing demand trend can be observed. According to recent report from the International Council of Marine Industry Associations (ICOMIA), around 30 million of recreational craft are in ownership across the world, with more than 5 million boats produced in 2017, which represents an increase of 10% compared to previous year (ICOMIA, 2018). However, it is expected that this market will face a slowdown, as well as other automotive and aerospace industries regarding the world pandemic crisis in the beginning of 2020. During the last six decades, composite boatbuilding sector has proliferated noticeably in particular for high-end applications like defence and transport. Regarding the tremendous technological advancements in composite sciences since the late 70s, composites began to get commercialised in a variety of marine end-users industry like sports and pleasure boats. The latter has been a major consumer of composite materials, with over 80% of pleasure boats in Norway that are made of GFRP (Eklund, 2013). In fact, the use of composites enables 30-40% reduction in overall weight in contrast to aluminium or steel, leading to a number of benefits like lower operating costs, higher fuel consumption efficiency and so reduced greenhouse gas emission (Dokos, 2013). Further advantages of using composites in

boatbuilding is the design freedom that is offered to boat architects regarding the possibility of manufacturing complex shaped parts with optimised fibre orientations and alignment to better withstand complex operating loads. Synthetic glass and carbon fibre have been used as reinforcement to unsaturated polyester and vinylester resin in pleasure boat construction over last decades. For more advanced use like large boats and impact critical applications like defence, sports vessels and catamarans, epoxy and vinylester resins are generally used with carbon fibres as reinforcement. These thermosets reinforced composites offer good lifetime cost due to better corrosion resistance and durability, but they present many processing and environmental drawbacks. Indeed, one of the biggest challenges posed by fibre reinforced composites, in particular in marine application, is their end-of-life (EoL) management (Oliveux et al., 2015).

Given the estimated high usage of FRP in boatbuilding, and with a boat lifespan of 30-45 years, around 140000 recreational craft are expect to reach their end-of-life every year (Önal and Neşer, 2018), with over 13000 only in France, which represents more than 5% of annual increase (Monier et al., 2016). In the Nordic countries, the number of boats is estimated at about 3 million, of which about 6% are above 40 years old (Eklund, 2013). The increase in marine boat production implies the increase of off-cuts during manufacture and EoL boats issues, which requires efficient waste management routes. Historically, the main waste management options for composite waste have been landfilling and incineration (Rybicka et al., 2015). Meanwhile, environmental legislation is becoming more and more restrictive. In fact, EU directive on landfill waste (1999/31/EC) reduced the permitted amounts of organic materials in landfills. In addition, the directive on waste incineration (2000/76/EC) restricted the emission of pollutants coming from waste incineration and co-incineration. More recently, the Extended Producer Responsibility (EPR), defined as the producer's responsibility for a product is extended to the post-consumer stage of a product life cycle, included pleasure and sports boats waste in French market. Therefore, EoL solutions for marine composite waste became limited. In addition, the environmental impact of composite waste disposed in landfills or illegally drowned in sea water is accelerating the urgency to reach environmentally viable routes to firstly deal with existing increasing composite waste from EoL boats, and secondly to find a way of designing new sustainable and valuable FRP vessels. In a recent study, it was found that landfilling and incineration of composite waste have nearly similar impact on climate change, fossil resources, ecosystem quality and human health (Witik et al., 2013). As a consequence, waste management of composites in the industry will be impacted as composite producers will need to look for alternative ways of processing by creating opportunities to explore novel composite sustainable design and more efficient industrial scale recycling strategies. In this scope, in regards to design alternatives, the marine composite market has witnessed some attempts to introduce novel bio-based and thermoplastic resins, natural fibres and eco-friendly sandwich panels in boat structure manufacturing. But a wide range of mechanical, durability and processability limitations withstand against the development of those methods.

1.2. Fibre reinforced plastic boat's end of life

As for CFRP market, the need to recycle GFRP raises from the increasing EoL large structures as wind turbine blades and marine boats. The actual situation of recycling of EoL marine FRP boats was studied by Eklund (Eklund, 2013), Önal et al. (Önal and Neşer, 2018), Singh et al. (Singh et al., 2010) and Jayaram et al. (Jayaram et al., 2018). The main recycling system for EoL boats is mechanical crushing. After collection of the boat from the owner and decontamination (removal of hazardous materials, oils, batteries and explosive materials) boats are crushed to an optimal size of around 40 mm. The salvaged small parts are then either burned in furnace and the remaining glass fibres end up as landfill, or co-incinerated to produce energy or used as aggregate in construction field. These techniques are adopted in Nordic countries (Finland, Sweden, Norway and Denmark) and also in France, via the APER, which is the only state approved establishment responsible to collect, dismantle and reduce FRP boats. The use of recyclates from mechanical shredding of FRP boats in a second-end use with other polymer or cement matrix cannot be evaluated separately due to lack of market size information. Other recycling techniques as thermal and chemical recycling use for GFRP recycling from specific FRP boats are not documented.

1.3. Fibre reinforced plastics recycling techniques

The recycling of thermoset composites in general has been the trend in the past two decades regarding the increasing waste flux and costs of raw materials. Recycling techniques could be classified in three main groups depending on the method: Mechanical, thermal and chemical recycling. Firstly, mechanical recycling involves the grinding or milling of FRP waste into progressively smaller sizes to produce fine powder, to be used as fillers, and coarser as fibrous products. The recyclates have a potential valorisation as fillers in injection or compression moulding with thermoplastic polymers, in sheet moulding compounds (SMCs) with thermoset resins and as reinforcement for cement and concrete for civil engineering applications. This technique is mainly used with GFRP not only for its simplicity and technical viability, but also for its efficiency and profitability. In fact, reducing large waste composite structures into usable dimensions is time and energy consuming steps. Added to the expensive required machinery and further transformation processes costs, consideration should be given to the balance of benefits, as virgin glass fibres are more or less cheap products, and short recycled glass fibre aspect ratio possess a relatively low market value. However, this method is less suitable for CFRP waste, as CF surface is harmful during crushing process and may cause attrition of the machinery, increasing then the operational cost and reducing the benefits margin as the mechanical strength of short reclaimed CF is largely altered. In addition, CF in production waste and EoL products still have significant economic residual value. Therefore, limited research and development studies focuses on the recycling of CF by the mechanical process (Kim et al., 2017; Verma et al., 2018). Moreover, thermal recycling processes include combustion, co-incineration, pyrolysis, fluidized bed and molten salt pyrolysis, etc. In those techniques, the FRP is exposed to high temperature in order to

decompose the matrix under oxidant or inert atmospheric conditions. The temperature to be used with most of thermal processes for thermosets lies between 450 °C and 700 °C, depending on the matrix thermal properties. The products of thermal processes are generally composed of a solid fraction, which includes reinforcement and fillers, with a potential char formation. The resin matrix is transformed to a gas state, with condensable phase that can be reclaimed in liquid form, and non-condensable light gases. This technique is largely used for CFRP. Depending on processing conditions, i.e. temperature and atmosphere, the quality of reclaimed carbon fibres could be different (Pimenta and Pinho, 2011). Pyrolysis is the most common technique in use at the industrial scale. It has been extensively considered by research studies to develop techniques as the fluidized bed (Pickering et al., 2015), microwave assisted pyrolysis (Amaechi et al., 2020) and vapo-thermolysis (Boulanghien, 2014; Ye, 2012). The third technique for recycling FRP is the chemical recycling, which consists of the use chemical solvent for the degradation and dissolution of polymer matrix and then to reclaim reinforcement. It mainly includes direct solvolysis and supercritical fluid methods. It is known that chemical recycling method allow the recovery of better-quality CF than mechanical or thermal recycling methods, but with high costs and bad environment footprint regarding the use of toxic solvent (Chen et al., 2019). Some techniques use supercritical, subcritical, and near-critical conditions (temperature and pressure) for the chemical degradation of the polymer matrix (Knight et al., 2015). In this particular conditions, the reclaim of reinforcement can be performed with less hazardous solvent as water and NaCl solution or a mixture of other solvents. Recently, new electrochemical technique using high voltages fragmentation method to disintegrate polymer matrix from reinforcement has been developed (Mativenga et al., 2016). Despite its better efficiency to reclaim longer and cleaner fibres, the chemical recycling technique is of a limited use in industrial-scale due to expensive required equipment that can resist to high pressure and temperature levels with the presence of corrosive solvents (Zhang et al., 2020).

1.4. Recycled carbon fibre market overview

All these techniques are used to recycle both glass and carbon fibres from production scrap, off-cuts and EoL products. A particular interest is given for carbon fibre reinforced thermoset composite which are of real economic and environmental interest to recycle due to their non-renewable fossil raw components and high energy consumption transformation steps (Oliveux et al., 2015; Pickering, 2006). For example, recycled carbon fibres (rCF) from ELG Carbon Fibre's cost is around 40% less than industrial virgin carbon fibre. Some other industrial suppliers announced that their rCF is from 20% to 40% less expensive than virgin carbon fibre (vCF). For Boeing, carbon fibres could be recycled at approximately 70% of the cost to produce vCF by using only around 5% of the required electricity ("Carbon fiber reclamation: Going commercial," n.d.). According to a recent market report, the cost-effectiveness, energy efficiency, lightweight and environmental sustainability are driving the rCF market growth, which is forecasted to reach USD 109 million in 2020, and projected to USD 193

million by 2025. The major composite recycling companies in production at industrial scale are ELG Carbon Fibre (UK), Carbon Conversions (USA), SGL Automotive Carbon Fibres (USA-GE) and Toray Industries (JP) (Zhang et al., 2020).

1.5. Positioning of the problem

The EoL issue is also to take under consideration for CFRP boats, as this material in widely used for advanced defence and sports boats such as cruise sailing yacht. As the market forecast an increase of EoL carbon fibre composite waste from several applications such aerospace, automotive and sports, it seems necessary to redesign products used in advanced boatbuilding sector for example, especially with no viable industrial scale-recycling route. Therefore, the development of more sustainable materials for marine application is an important on-growing research area. The newly developed reactive methacrylate thermoplastic resin Elium® from ARKEMA presents an alternative to thermoset resins currently used in composites for marine structures. It can be processed at room temperature with processing techniques typical of thermosets, like RTM and resin infusion. This thermoplastic resin reinforced by carbon fibres presents good mechanical and durability properties, compared to a carbon fibre reinforced vinylester composites (Davies et al., 2017). The recyclability potential of Elium resin arises from its micro-molecular structure, mainly composed by methyl methacrylate (MMA) monomer, which could facilitate the recycling of large-scale composite parts by recovering and reusing initially used raw materials (Cousins et al., 2017). As far as we know, only one previous research has investigated the recycling and reuse of an Elium based composite for wind turbine blades. Four methods were applied by Cousins et al. (Cousins et al., 2019) in order to quantify and demonstrates the ways to recycle large-scale glass fibre-Elium thermoplastic resin composite parts by recovering and reusing material from a component of a wind turbine blade. The lab-scale recycling techniques used were thermal decomposition of the polymer matrix, mechanical grinding, thermoforming, and chemical dissolution. Preliminary results from mechanical and economic analysis showed a particular good interest of chemical recycling by dissolution among other recycling methods.

Herein, the aim of this study is to demonstrate the advances in the way to recycle an acrylic thermoplastic reinforced carbon fibre composite intended to a marine environment use. CF/Elium panels were produced by resin infusion and then depolymerised. Both reinforcement as well as matrix were recovered at kg-scale and reused to re-manufacture long carbon fibre composites. Pyrolysis technique was employed to depolymerise the matrix and recover both CF and condensed monomer, which was purified to remanufacture recycled Elium resin. In order to study the efficiency of this process, Gas Chromatography analysis were conducted on raw and purified recovered monomer. The performances of recovered constituent materials were evaluated at fibre and composite scales. Thermogravimetric analysis TGA, SEM observations as well as surface tension were performed on virgin CF (vCF) and recycled carbon fibres (rCF). Semi-recycled composites made from rCF and virgin Elium (vElium) and fully recycled composites made from rCF and recycled Elium resin

(rElium) were remanufactured by resin infusion and their properties were compared to reference material. Mechanical properties were assessed by tensile, interlaminar shear and dynamic mechanical analysis tests.

2. Materials and methods

2.1. Material under investigation

The material under investigation in this study is an acrylic matrix and carbon fibre reinforced laminate composite. The Elium 188-O resin was kindly supplied by ARKEMA and the reinforcement was a stitched biaxial carbon fabric Cbx600 24K T620 from Sicomin. The Elium 188-O resin is a polymer solution of methyl methacrylate (MMA) monomer and of acrylic copolymers, having a viscosity of 100 cPs and activated by a benzoyl peroxide (BPO) thermal initiator from AkzoNobel. The glass transition temperature given in the product datasheet is about 109 °C. The Non-Crimp balanced biaxial carbon fibre fabric has around 627 g/m² of areal weight, with two plies of +45° and -45° fibres directions. The compatibility of the fabric, according to the manufacturer, is for general use like epoxy, polyester and vinylester use. Therefore, no specific sizing for acrylic resin is used. Laminate composites of 4 plies of CF fabric of 450×420 mm^2 were produced by resin infusion method at room temperature. For each ply, fabric weight and dimensions were carefully measured to calculate the apparent areal density, which was found to be around 640.5 g/m². During polymerisation, an exothermic reaction took place characterized by a temperature peak. After demoulding, no special post-curing was performed on infused plate, which were conditioned at 23 °C and 50% RH. The average thickness of the 4 ply infused laminate is around 2.5 mm. Density measurements on a Micromeritics gas pycnometer (AccuPyc 1330 model) with helium gas were then conducted on samples of 35×12×2.5 mm^3 at room temperature in order to calculate the apparent fibre and matrix volume fraction according to ASTM D317–15 standard. The measurements were conducted on at least three samples. The void volume fraction is deduced from fibre and matrix volume fraction. The fibre volume fraction V_f (%) is calculated using Equation 1below:

$$V_f = \frac{W_f}{\rho_f \times V_c} \times 100 \qquad \text{Equation 1}$$

Where ρ_f is the fibre density (1.7 g/cm^3), V_c is the composite volume (m^3) and W_f is fibre weight (g), calculated using Equation 2.

$$W_f = A_w \times N \times L \times l \qquad \text{Equation 2}$$

Here, A_w is the fabric areal weight ($g.m^{-2}$), N is the number of plies, L and l are the composite sample length (m) and width (m) respectively. Equation 3 gives then the resin volume fraction V_r :

$$V_r = \frac{W_c - W_f}{\rho_r \times V_c} \times 100 \qquad \text{Equation 3}$$

With W_c is the composite weight (g) and ρ_r is the resin density (1.17 g/cm^3). The void volume fraction V_p is finally calculated using Equation 4:

$$V_p = 100 - V_f - V_r \qquad \text{Equation 4}$$

The results from infused laminates are then presented in Table 1.

Table 1 : Calculated constituent volume fraction of infused laminates

Properties	Fibre volume fraction v_f	Matrix volume fraction v_m	Void volume fraction v_v	Fibre weight fraction
Measurement [%]	61.9 (0.53)	36.6 (0.51)	1.5 (0.02)	70.9 (0.39)

Standard deviations are given between parentheses

2.2. Characterisation methods

2.2.1. Scanning Electron Microscope

Scanning electron microscopy can provide more detailed information on the matrix, fibres and fibre/matrix interfaces in the case of composite laminates. A FEI Quanta 200 FEG was used for images acquisition. To do so, polished sections were prepared by casting a polymer in a specimen holder. After polymerisation, the top surface of the samples was polished and a thin carbon foil was applied using a Balzers CED030 metal coater. Moreover, to observe fibre surface and to perform diameter measurements, a carbon fibre bundle is placed on a conductive carbon adhesive tape. The adhesive tape is then positioned in the top of an aluminium specimen holder.

2.2.2. Thermogravimetric analysis

The thermogravimetric analysis (TGA) technique consists in measuring the variation in mass of a sample as a function of time or temperature in order to analyse its thermal decomposition and to determine its thermal degradation (or stability) temperature. The machine used is a Setaram (SETSYS Model). Samples with a mass between 10 and 15 mg are placed in ceramic crucibles. The purge is carried out with a nitrogen flow of 40 mL/min. The measurement protocol consisted first of all of stabilization for 30 minutes at 30 °C followed by a temperature ramp between 30 and 900 °C at different heating rates: 2, 5, 10 and 20 °C/minutes.

2.2.3. Mechanical tensile test

Axial tensile test specimens were machined from the infused plates using a water-cooled diamond saw. 250×25×2.5 mm^3 specimens were cut from the composite panels and 50×25×2 mm^3 aluminium tabs were bonded at each specimen ends using Loctite Super Glue 3 commercial adhesive. Regarding the limited dimensions of recycled carbon fibre fabric, tensile specimens of semi-recycled and full recycled composites were cut to the half of nominal tensile specimen dimension and therefore they were 125 mm length and 12.5 mm width. The aluminium tabs were also half dimensions (25×12.5×2 mm^3). Verification of the suitability of this sample geometry change with reference material will be presented in results section. Prior to testing, all samples were kept at 25 °C and 50% RH. All tests were performed at a crosshead speed of 1 mm/min according to ISO 527-4 standard requirements on an MTS Criterion C45.105 tensile machine equipped with a 100 kN load cell. The in-plane strain tensor was evaluated using full-field Digital Image Correlation (DIC) on initially painted and speckled samples. Using a LabVIEW software, simultaneous images and load data are recorded from the tensile machine. Further image analysis was performed using an in-house image correlation software in order to extract deformation data and thus mechanical properties of the materials.

2.2.4. Interlaminar Shear Strength ILSS

The short-beam test method was used to monitor the quality of fibre/resin bond in the interphase area by mean of failure resistance calculations and failure modes observations according to ASTM D2344 / D2344M standard. For this test, specimens were cut from 5 mm thick laminates (8 plies of carbon fibre fabrics). The aim is to obtain a span length of around 20 mm. The load was applied at 1 mm/minute on load cell of 10 kN and an accuracy of 0.1 N on a Zwick-Roell testing machine (model Z010/TH). The apparent interlaminar shear strength τ, expressed in MPa, is calculated using the following equation:

$$\tau = \frac{3}{4} \times \frac{P_m}{b \times h} \qquad \text{Equation 5}$$

where: P_m is the maximum load observed during the test (N), b and h are the measured width and thickness (mm), respectively.

2.2.5. Dynamic Mechanical Analysis

DMA tests were conducted in order to study the temperature effect on composite and neat resin specimens having dimensions of 80×10×2.5 mm^3 and 80×10×2 mm^3, respectively. The dual cantilever beam testing mode is used accordingly to ASTM D5418-15 on a METRAVIB DMA50 machine with a free span length of 27 mm on each side. The tested specimens were machined from infused plates in the longitudinal direction of the fibres using a water-cooled circular diamond saw. Tests to ensure the linearity of the response were previously conducted at different solicitation frequencies and dynamic displacements. A 5 Hz frequency, 10 μm dynamic strain amplitude and temperature range from 40 to

160 °C at a heating rate of 3 °C/min test parameters were finally chosen. The storage modulus, loss modulus and loss factor data were directly collected from testing machine.

3. Results and discussion

3.1. Composite pyrolysis

The aim of this section is to describe the depolymerisation method developed by ARKEMA in order to recover clean CF as well as the Elium monomer as recycled products. The depolymerisation tests were performed at ARKEMA's laboratory (CRRA, France).

3.1.1. Composite sample preparation and reactor description

In order to optimise the filling of the reactor regarding its volumetric capacity and dimensional restrictions, three types of discs were machined from infused plates: Flat discs of 142 mm and 137 mm diameter and drilled discs of 137 mm diameter with a 10 mm hole in the centre. Six discs were cut from each infused plate using a water jet machine as presented in Figure 1.a. The obtained discs are then dried for 24 hours in order to eliminate remaining water (Figure 1.b) and then stored at room temperature.

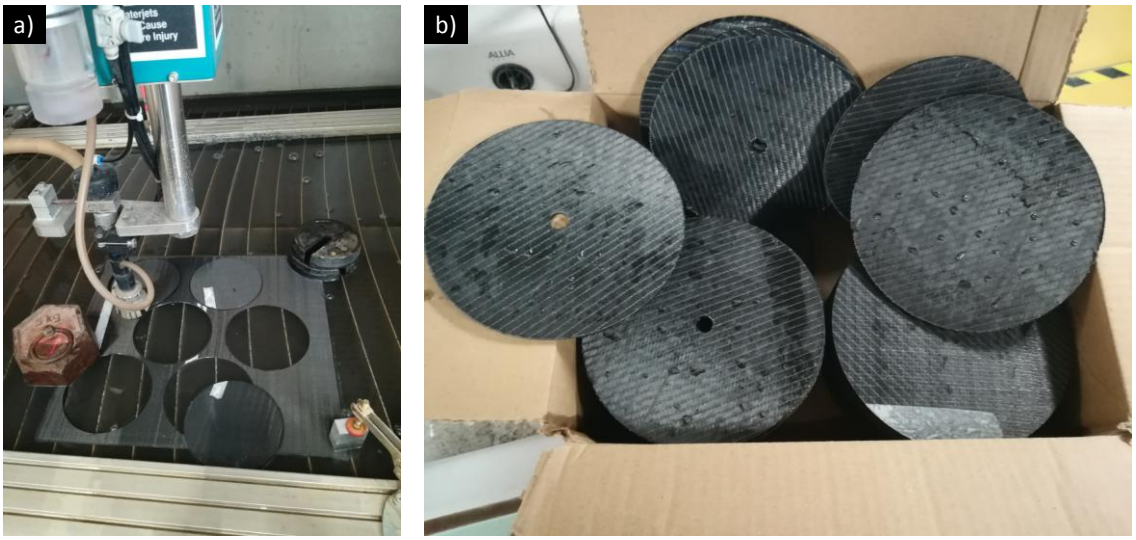

Figure 1: Water jet cutting machine (a) and discs cut with the desired diameter (b)

The overview picture of pyrolysis apparatus is presented in Figure 2.a. A 4.5 L stainless steel cylindrical reactor (Figure 2.b) is equipped with electrical resistances fixed on its outer surface and is covered with a heat insulator to minimize heat dissipation. The reactor is equipped with several thermocouples in order to measure temperature at different locations, including the centre of the reactor and then to regulate the heat according to the temperature set point via a regulator. All the sensors and valves are directly related to a central command, from where the full program of the depolymerisation process steps and its parameters can be defined. The gas phase of the reactor is connected to a liquid receiving flask via an insulated and cooled condenser at 5 °C.

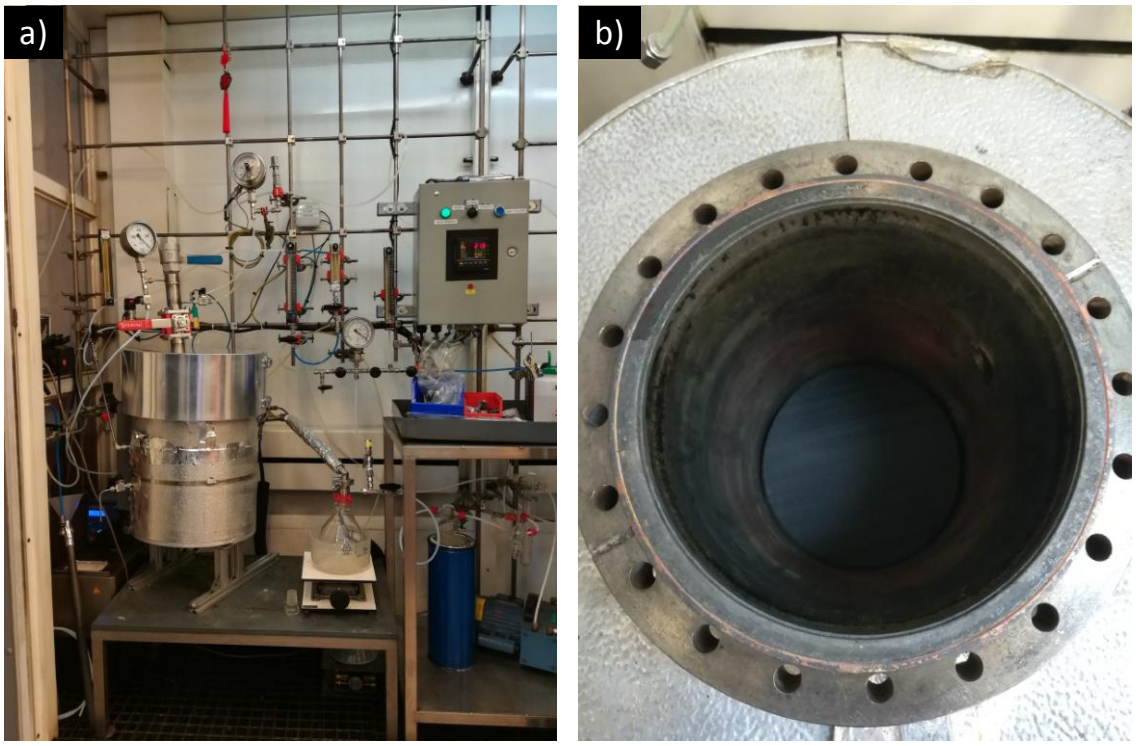

Figure 2: Reactor overview (a), filling the bottom of the reactor (b)

Around 30 discs are stacked one by one until reaching a level where discs are inserted around the central thermocouple. The filled final weight of composite is hence around 1500 g.

3.1.2. Details and outputs of depolymerisation process

Once the reactor is filled with composite discs, the heat insulator cover is installed and the upper reactor part is tightened firmly with bolts. After purging the reactor with nitrogen, the reactor is heated for more than 4 hours at different temperature levels around 350-450 °C. Condensed vapours are progressively recovered in the liquid receiver flask while depolymerisation proceeds. The recovered monomer liquid is then stabilised using hydroquinone as a polymerisation inhibitor. Once the reactor has reached room temperature, the reclaimed carbon fibre residue was collected in the reactor.

Table 2: Depolymerisation process results

Depolymerisation run	Introduced composite weight [g]	Reclaimed carbon fibre weight [g]	Reclaimed crude MMA weight [g]	Solid residue fraction [% vs initial composite weight]		Liquid residue fraction [% vs initial composite weight]	Material balance [%]
1	1577	1137	394	72.1		25.0	97.1
2	1634	1177	428	72.1		26.2	98.2
Total	3211	2314	822	*Average*	72.1	25.6	97.7

Two depolymerisations were conducted on the CF / Elium 188-O composite in order to recover sufficient monomer quantity for further tests. The experimental details about both depolymerisations in terms of weight of recovered fibres and crude MMA monomer are given in Table 2. Both depolymerisation test results are superimposable, particularly for the solid residue fraction, which represents 72.1 % of initially introduced composite weight. The average results of the material balance before and after depolymerisation is 97.7 %. The loss of material is due to non-condensable gases (estimated to be between 0.3 and 1.2%) and residual oily liquids, which remain stuck to the reactor interior wall and condenser pipe.

The reclaimed carbon fibres discs and crude MMA pictures are presented in Figure 3.a and Figure 3.b. The main advantage of static heating is that the initial length and orientations of fibres are not modified during the pyrolysis. In order to qualitatively evaluate the efficiency of the process at the top and middle of the reactor, the mass of two discs was recorded before and after depolymerisation. It was found that the solid residue fraction in the top of the reactor was slightly higher than the middle region (72.0% compared to 70.8%, respectively), which is likely due gradient of temperature in the reactor due to thermal transfer. It is noteworthy to mention that we visually observed the total degradation of stitching polyester fibre that was initially present in the CF fabric with an areal weight of 9 g/m². The major visual differences between virgin and recycled carbon fibre fabric is their aspect as the recycled discs are more rigid and compacted and with a brilliant surface.

The reclaimed crude liquid had yellow-orange colour as presented by Figure 3.c. As the Elium 188-O is mainly formed by MMA monomer (more than 70% according to the safety data sheet), an analogy with the thermal degradation of PMMA under inert atmosphere can be proposed. Many works have treated the pyrolysis of PMMA under inert atmosphere and found that it depolymerises by releasing the methyl methacrylate monomer (MMA) with excellent chemical yield. Ferriol et al. described that thermal degradation of PMMA occurs by a chain radical mechanism initiated by four different initiation steps depending on end chains nature, defects in the chain and random scission (Ferriol et al., 2003). A study of the thermal decomposition of Elium resin (grade 150) was recently published by Raponi et al. (Raponi et al., 2018) in which TGA were conducted on resin samples with different

initiator contents. A three steps degradation mechanism was adopted to explain the thermal decomposition of Elium 150 resin and temperature intervals were given to each step. The works of Cousins et al. (Cousins et al., 2019) also describes pyrolysis of Elium resin in TGA study leading to conclude that the acrylic matrix system is advantageous in the case of pyrolysis of large-scale composite parts as wind turbine blades . In a recent study, the depolymerisation of PMMA was investigated using thermogravimetric analysis coupled with mass spectrometry (TGA-MS) method. Authors reported that the degradation was initiated by homolytic scission of a methoxycarbonyl side group by a random scission degradation. During the degradation process, a number of small radicals can be formed via disproportionation, and they cannot be depolymerised efficiently thus giving rise to the generation of by-products. The degradation temperature, initial molecular weight and the presence of oxygen may be also responsible of the generation of by-products during polymer degradation (Godiya et al., 2019).

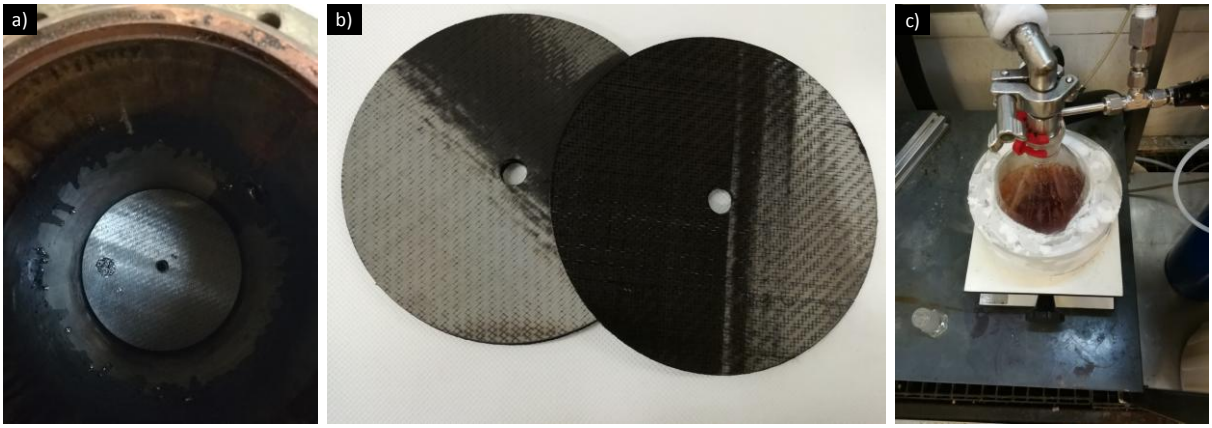

Figure 3 : Recycled carbon fibre inside the reactor (a), after extraction from the reactor (b); Recovered liquid crude MMA monomer (c)

3.1.3. Chromatography of reclaimed substance (MMA), distillation technique

As reported in literature (Kaminsky and Franck, 1991), crude MMA obtained by PMMA depolymerisation contains many by-products. Analysis of the reclaimed liquid of present study was performed by gas chromatography with flame ionization detection. Quantification of MMA content in crude MMA using an internal standard was found to be 77% and 72% for respectively first and second depolymerisation tests. Main identified by-products are methyl isobutyrate, ethyl acrylate, methyl acrylate, methacrylic acid and methanol. Many heavier compounds were detected, but have not been identified. Table 3 represents a quantitative summary of the depolymerisation products of both test runs. By taking into account the weight of crude MMA that has been recovered and its purity, we calculated that 19 g of MMA is recovered per 100 g of composite in both trials meaning identical yields in MMA. In the second trial more liquid was recovered, but MMA purity was slightly lower because more heavy impurities were collected than in first trial.

Table 3: Quantitative summary of two depolymerisations MMA and by-products

	Depolymerisation 1	Depolymerisation 2
MMA purity (%) (with internal standard)	77	72
MMA (% area)	82	78
Methanol (% area)	1.8	1.8
Methyl acrylate (% area)	0.11	0.12
Methyl propanoate (% area)	0.06	0.08
Ethyl acrylate (% area)	0.15	0.15
Methacrylic acid (% area)	0.06	0.08
MMA weight / composite weight [%]	19	19

Crude MMA from both depolymerisation trials was then distilled in a packed distillation column with reflux head presented in Figure 4.a. From 703 g of crude MMA at 75% purity, 385 g of MMA with 99.5% GC purity was recovered. A picture of crude MMA before distillation and MMA with high purity is given by Figure 4.b. The purified recycled MMA monomer was formulated by ARKEMA (GRL, France) to finally obtain around 500 g of recycled Elium 188-O resin (denoted here rElium) as presented in Figure 4.c. This quantity of rElium was then used to cast neat resin samples and composite plates by resin infusion method.

Figure 4: (a) Used vacuum distillation setup, (b) distillation input liquid (dark) and distillate (transparent) and (c) Recycled Elium 188-O (rElium) resin obtained from polymerisation of recycled MMA

3.2. Composite remanufacturing processes

Reclaimed carbon fibres from depolymerisation have conserved their original length and orientation during the process. The recycling method allowed the recovering of 72.1% of initial introduced composite weight. While manufacturing the composite panels it was found that fibre weight fraction average from all cut plates was 70.9% (0.38). The difference may be simply related to a residual polymer on fibre surface or between adjacent fibres or stacked fabric plies. As the re-polymerised Elium resin quantity was limited (around 480 g), an optimisation in resin infusion lay-up was mandatory to reinfuse rCF / rElium totally recycled composite

3.2.1. Optimisation of infusion technique for rCF discs

As rCF fabric geometry is predefined as circular geometry, the infusion layup was adapted in order to insure full wettability and minimum resin consumption. Major changes between vCF infusion and rCF infusion is the diameter of both infusion pipe and spiral as well as the presence of peel ply at the top and bottom of the rCF fabric as presented in Figure 5. In fact, first attempts of rCF resin infusion revealed that the bottom surface of infused rCF/Elium discs had some dry spots. This was related to the high rigidity and so low compaction ability of the rCF fabric. When vacuum is applied during resin infusion, more compaction leads to difficulties of the resin to reach some points at the bottom surface compared to top surface, where the peel ply and a flow mesh are present. The solution adopted is the use of peel ply at the level of the bottom surface i.e. between glass plate and rCF fabric layers. This lead to a slight increase in final infused disc thickness compared to the initial thickness of composite plates before depolymerisation. This additional thickness of about 0.25 mm is directly related to the surface roughness due to the peel ply. One can remark from Figure 5.b that the flow mesh disposition was also adopted to the circular geometry of rCF fabric to guarantee the quality of the laminate without internal weld lines.

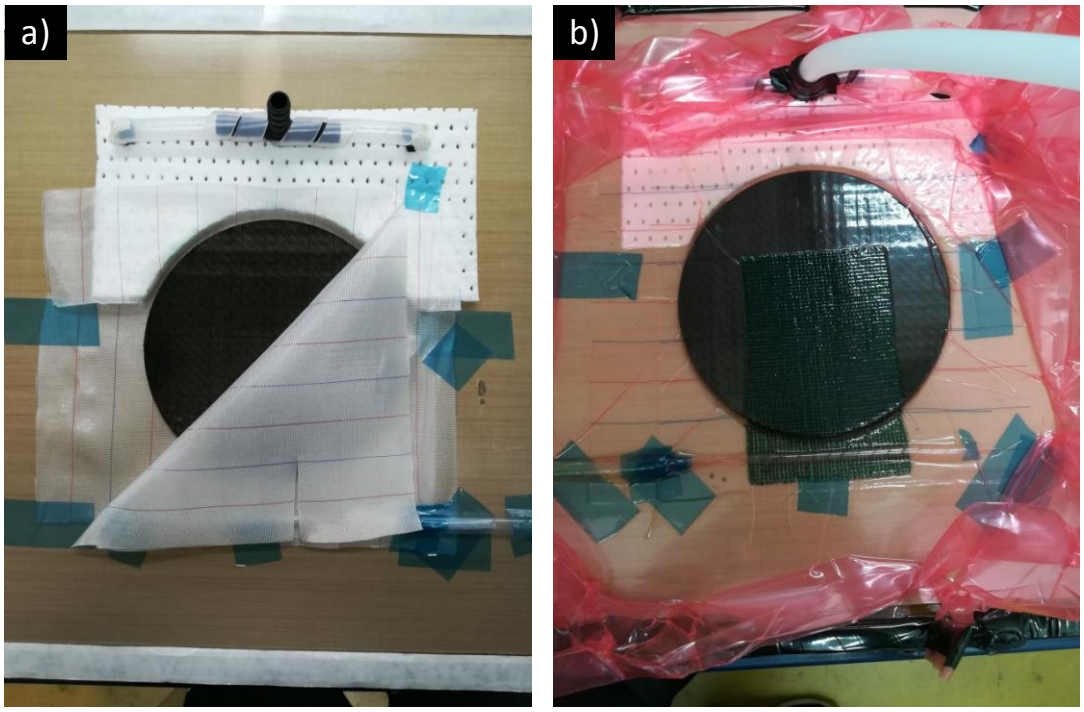

Figure 5: rCF/Elium resin infusion layup to optimise the process for circular fabric geometries (left) and infused composite disc (right)

Scanning Electron microscope and calculations of the components volume fractions were also performed in order to qualify the effect of using peel ply fabric on both top and bottom sides of rCF/Elium composites. To do so, two configurations of rCF/Elium composite discs were manufactured; the first with only peel ply and flow mesh on top side (standard method) and the second with peel ply fabric on top and bottom sides. Results from SEM imaging showed, when using peel ply on both top and bottom faces, a significant decrease in apparent voids at a cross polished section as presented by Figure 6. It is also worth noting that voids present in the microstructure were principally regrouped at the level of inter-ply matrix rich region.

Table 4: Constituent's volume fractions calculated to optimise the resin infusion layup for rCF discs

	Fibre volume fraction v_f[%]	Matrix volume fraction v_m [%]	Void volume fraction v_v [%]	Fibre weight fraction [%]
CF/Elium (reference)	61.9	36.6	1.5	70.9
rCF/Elium (1 peel ply)	57.3	39.3	3.4	66.7
rCF/Elium (2 peel plies)	56.1	42.4	1.5	66.1

These findings were confirmed by calculations of the components volume fractions using the Helium pycnometer and Equation 1- Equation 4 as presented in Table 4. An explanation of this significant difference in fibre volume fraction will be given in next section.

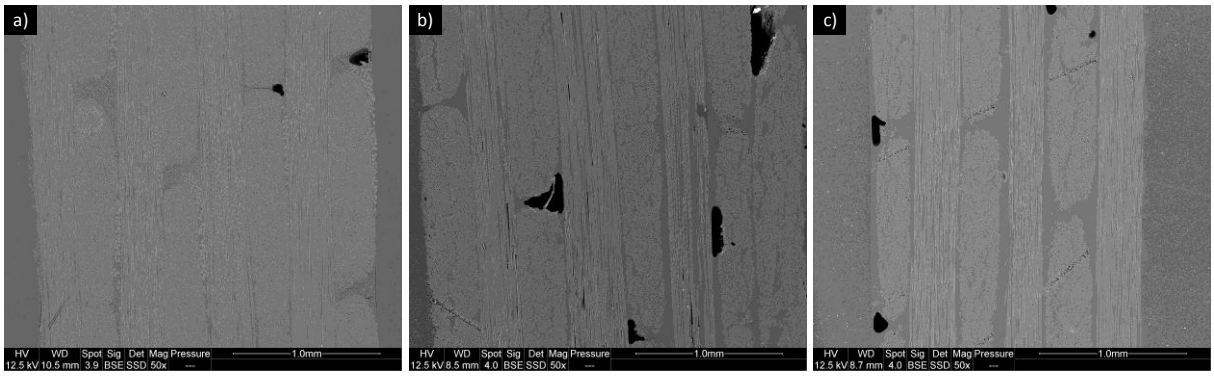

Figure 6 : SEM images with identical scale of polished section from : a) reference CF/Elium, b) rCF/vElium with peel ply on top side and c) rCF/vElium with peel ply at both top and bottom sides

3.2.2. Manufacturing of recycled composites

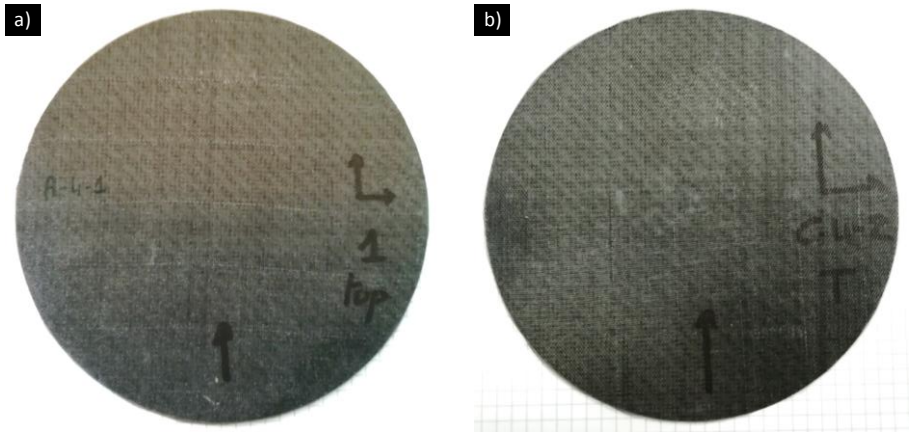

Figure 7 : Infused rCF discs : a) with virgin Elium resin and b) with recycled Elium resin

Recycled composite discs were manufactured by infusion technique. A total of three discs were infused for semi-recycled (rCF/Elium) and full-recycled (rCF/rElium) configurations. Two of them with 4 layers of rCF fabric (biaxial fabric) for tensile and DMA test samples. The third plate had 8 layers of rCF fabric and will be used for ILSS test. A picture of a rCF/Elium and rCF/rElium discs are presented in Figure 7. Polished sections from composite samples were prepared for SEM observations in order to investigate the quality of fibre/matrix bonding. Samples were cut far from edge regions for reliable observations. Results show a good bonding between fibres and matrix at two different magnitudes (Figure 8). In addition, one can remark the good wettability of particularly recycled carbon fibres as the resin correctly impregnated individual fibres. From pictures c, d, e and f related to rCF, one can remark the existence of resin reach areas inside one CF tow and at the interplay level. This could be related to the compaction difference, as virgin CF fabric were less stiff and a good compaction can be performed. For rCF fabric, the residual polymer on fibre surface lead to stiffer fabric and thus fibre tows are less compactable. In overall, an excess in resin can be distinguished for rCF based composites.

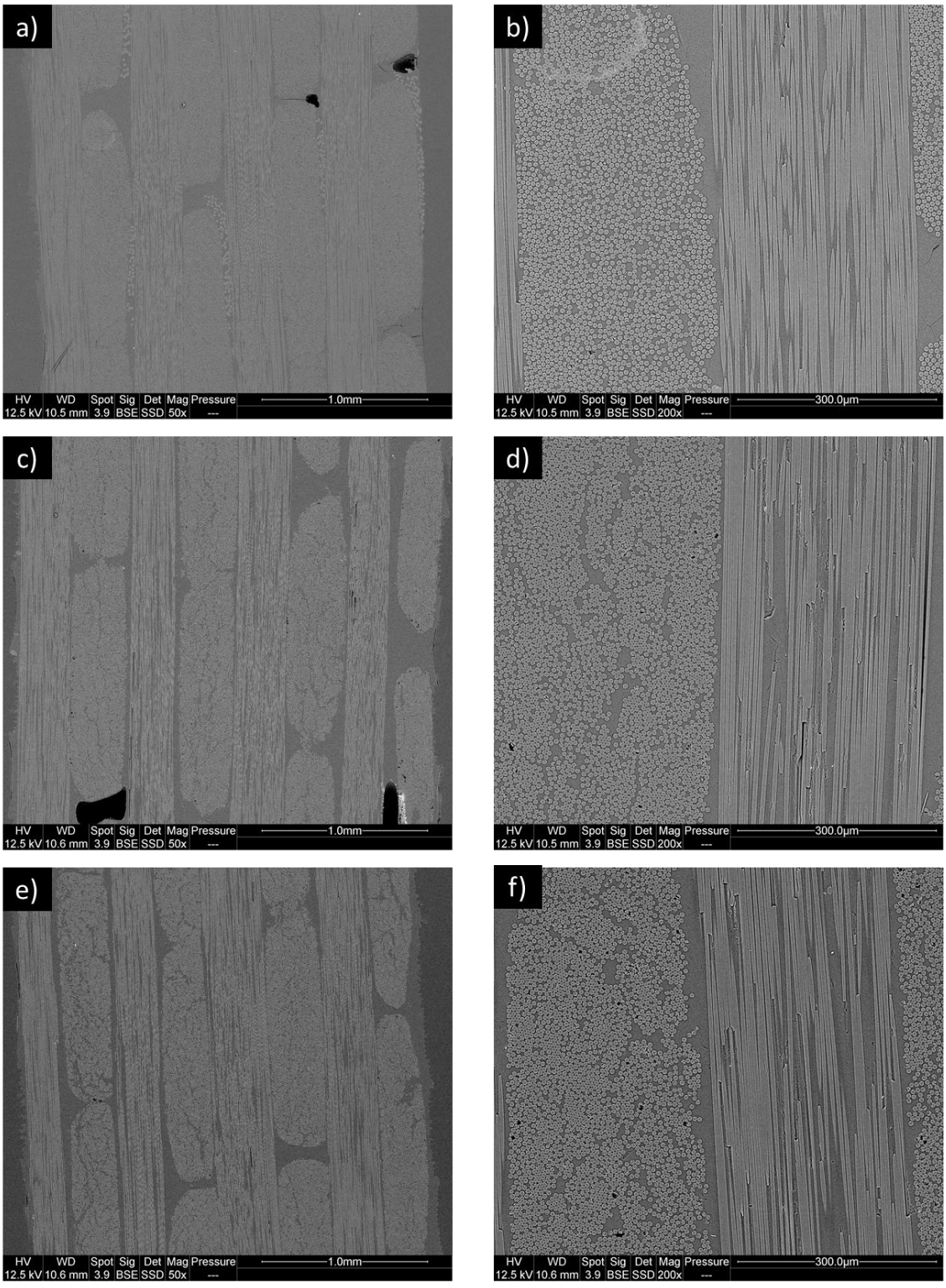

Figure 8 : SEM pictures showing the microstructure of: reference composite (a and b), rCF/vElium (c and d) and rCF/rElium (e and f)

Samples for density measurements were cut at random emplacement from virgin composite plate as well as semi-recycled and full-recycled discs. Using the above-mentioned standard, fibre and matrix volume fractions were calculated and void volume content was deduced for all studied composites.

The measurements were carried out on a total of 6 samples from two different plates for each configuration. Mean results and standard deviation are summarized in Table 5.

Table 5 : Results of the calculations of constituent's volume and weight fractions and the fabric areal weight

	Fibre volume fraction v_f [%]	Matrix volume fraction v_m [%]	Void volume fraction v_v [%]	Fibre weight fraction [%]	Fibre areal weight [g.m^{-2}]	Density [g.cm^{-3}]
vCF/vElium (reference)	61.9 (0.54)	36.6 (0.51)	1.5 (0.02)	70.9 (0.41)	640.5 (2.66)	1.53
rCF/vElium	54.8 (1.10)	43.6 (1.27)	1.6 (0.16)	66.4 (1.14)	631.4 (4.89)	1.49
rCF/rElium	55.4 (1.12)	42.9 (1.9)	1.7 (0.77)	67.1 (0.38)	628.2 (1.08)	1.50

Standard deviations are given between parentheses

As it was shown by SEM observations, discs with rCF presents higher matrix volume fractions compared to reference material. Subsequently, the difference can be observed on fibre volume fraction, which decreased from around 62% to 55%. It is known that, when a peel ply is used for infusion, an additional thin layer of bulk resin is formed at the surface directly in contact with the peel ply fabric. Furthermore, the total degradation of PET stitching fibre after depolymerisation led to more free volume between carbon fibre tows as it was observed on CF discs after depolymerisation and confirmed by areal weight measurements. In fact, the difference between areal weight measurements between vCF and rCF is consistent with the fabric manufacturer data, which evaluated the stitching fibre areal weight to 9 g/m². When infused, these free volumes were then filled with the matrix, which would partially lead to matrix rich areas and subsequently higher matrix volume fraction and lower fibre weight fraction compared to the reference composite. It is also worth noting that the void volume fractions are similar either for vCF or rCF composites. This is particularly important when investigating further mechanical properties. Moreover, density measurements on vCF and rCF were found to be very close (1.771 g/cm^3 and 1.781 g/cm^3, respectively). The same observations were found for vElium and rElium resins with a difference of less than 0.4% (1.177 g/cm^3 compared to 1.182 g/cm^3 for vElium and rElium, respectively).

3.3. Analysis of reclaimed fibres

3.3.1. Thermogravimetric analysis on fibres

The thermal stability of virgin and recycled carbon fibres was determined by thermogravimetric analysis (TGA). The TG and dTG curves are presented in Figure 9 for samples of vCF and rCF at

different heating rates: 2, 5 and 10 °C/min. From Figure 9.a, it can be noticed that, for each fibre type, the scanning rate had a negligible effect on the material response, as the curves are nearly superimposed. Furthermore, when comparing rCF curves to vCF, a major difference can be observed. However, vCF presented a first major weigh loss of around 1% between 250 °C and 420 °C, unlike rCF where no weight loss was observed between these two temperatures. These lead to a first assumption that, when depolymerised, carbon fibres have lost the sizing already present on fibre surface. According to fibre description from manufacturer, the sizing amount is 1% to control handleability and adhesion properties. The sizing type is not publically disclosed, but it is known that for a compatibility with epoxy, vinylester and unsaturated polyester resin systems, an organic polymer-based sizing is commonly used. This is consistent with the degradation temperature interval determined from TG curves. Derivative thermogravimetric curves are given in Figure 9.b as the rate of material weight changes upon heating. This technique is generally used in order to identify decomposition stages and peaks temperatures, which occur close together. For vCF, a significant peak took place at around 347 °C, which was related to thermal decomposition of the sizing. Compared to rCF presented by dashed curves, no peak related to weight loss was observed in same temperature interval as dTG curves for vCF, which indicates the thermal stability of rCF at this interval. By analysing the curves at higher temperatures, an acceleration of weight loss can be observed starting from around 620 °C indicating the damage of fibres. At all heating rates tested, the total weight loss of both vCF and rCF did not exceed 5% for a heating from 30 to 900 °C under nitrogen. This is in line with previous study by Feih and Mouritz (Feih and Mouritz, 2012) where thermal decomposition of T700 carbon fibres were investigates under nitrogen and air atmospheres. Findings showed the good thermal stability of T700 CF under nitrogen with around 0.8% of weight loss, contrarily to fibre oxidation under air. This similarity of thermal stability at higher temperature between vCF and rCF indicates a satisfactory depolymerisation efficiency at this level.

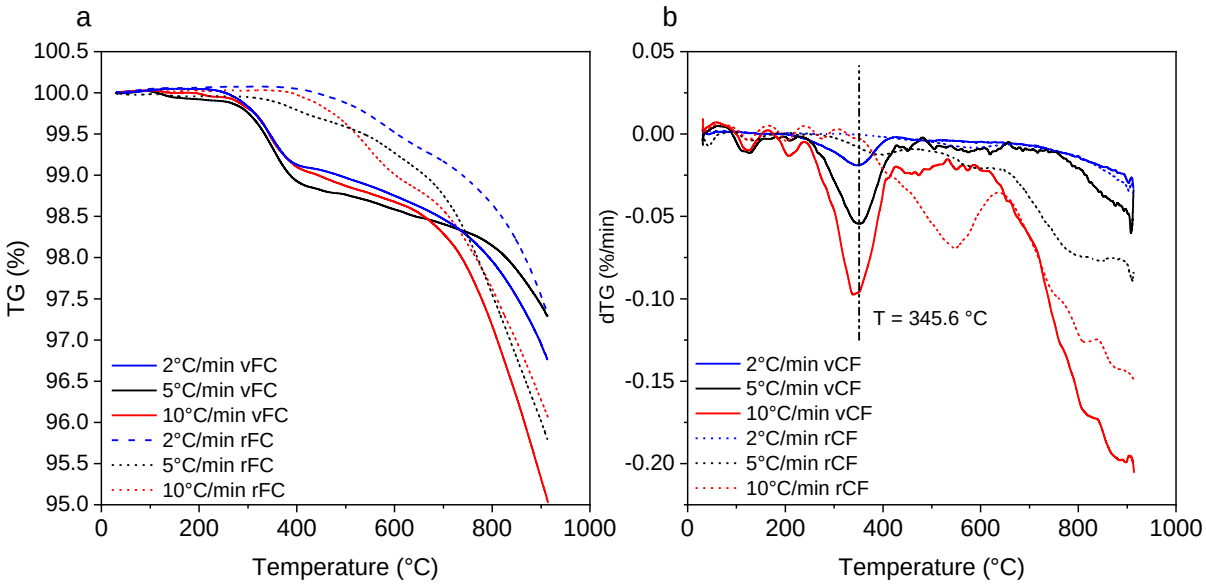

Figure 9: Thermogravimetric analysis (TG) and derivative thermogravimetric analysis (dTG) of vCF and rCF at 2, 5 and 10 °C/min scanning rates under nitrogen atmosphere

3.3.2. SEM on carbon fibres

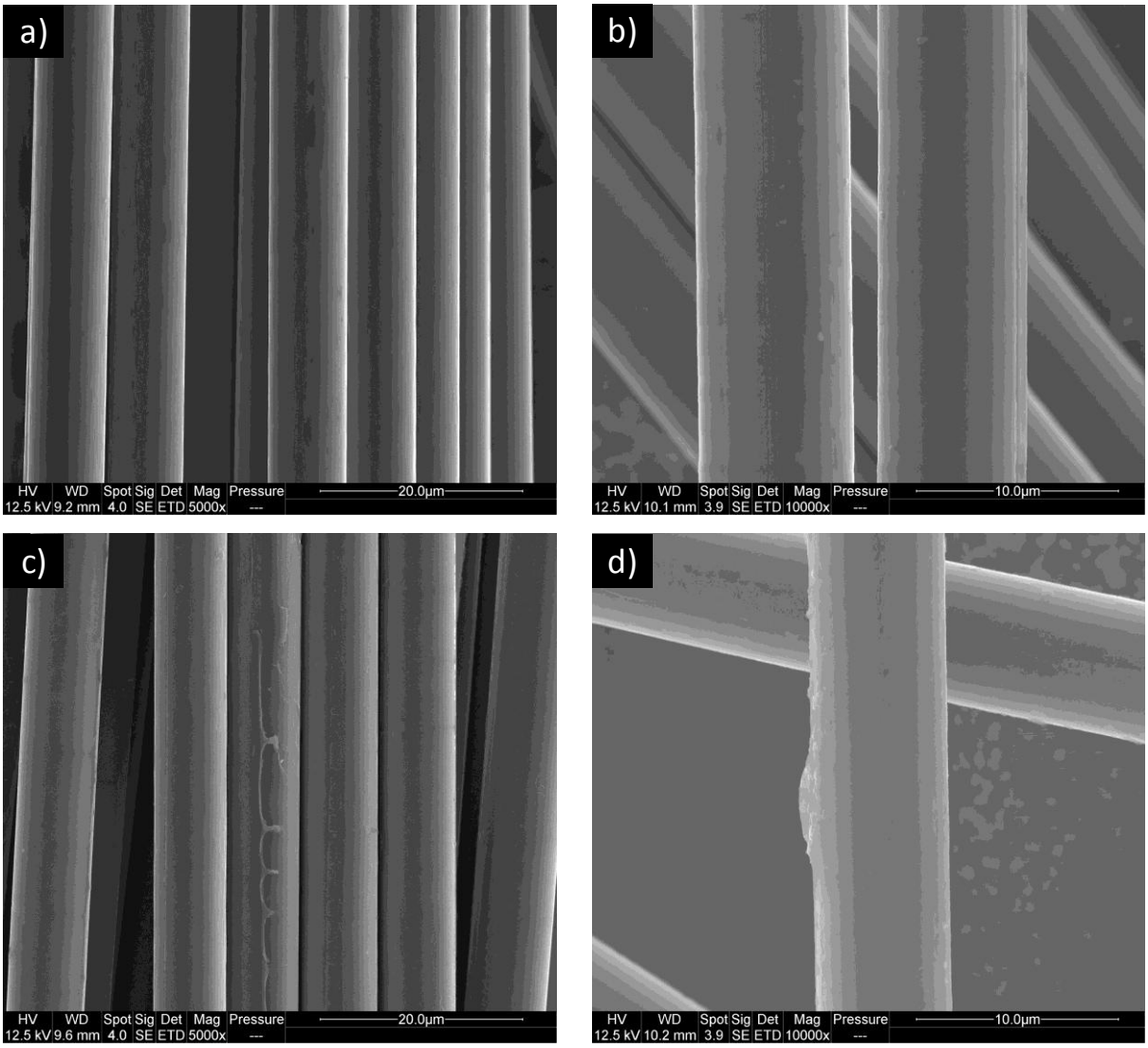

Figure 10 : SEM images of virgin (a and b) and recovered (c and d) carbon fibres

The reuse of recycled fibres in high-end applications is conditioned by the quality of the recovered fibres. SEM observations on fibre surface and diameter change may lead to some important results. Virgin and recycled carbon fibre surfaces were investigated by SEM and some of the characteristic micrographs are given in Figure 10. Images a and b show virgin fibre surface at two different scales. Results show the smooth surfaces of virgin fibres due to the coating of fibre surface by the sizing. For depolymerised fibres, it could be clearly seen that fibres have some residue patches adhered to the surface as shown in image c. Furthermore, the residual polymer is a local phenomenon as it is not coating the whole fibre surface (image d). In fact, they form longitudinal and discontinuous ridges. In order to qualify reliably the diameter loss after depolymerisation step, a large number of measurements was performed on virgin and depolymerized fibres. Diameter measurements on around 30 different vCF and rCF were conducted by SEM and the results are presented as histograms with normal distribution in Figure 11. A similar distribution trend can be observed but with a clear different mean values. vCF mean dimeter was 7.48 µm, while rCF mean diameter was found around 6.9 µm with a

close standard deviation between both measurements. This difference could confirm the TGA findings and hypothesis on sizing decomposition during depolymerisation of composites by pyrolysis process. These results lead to a first estimation of the sizing thickness on carbon fibre surface, which is found to be around 300 nm on 30 fibres evaluated from virgin and recycled carbon fibres.

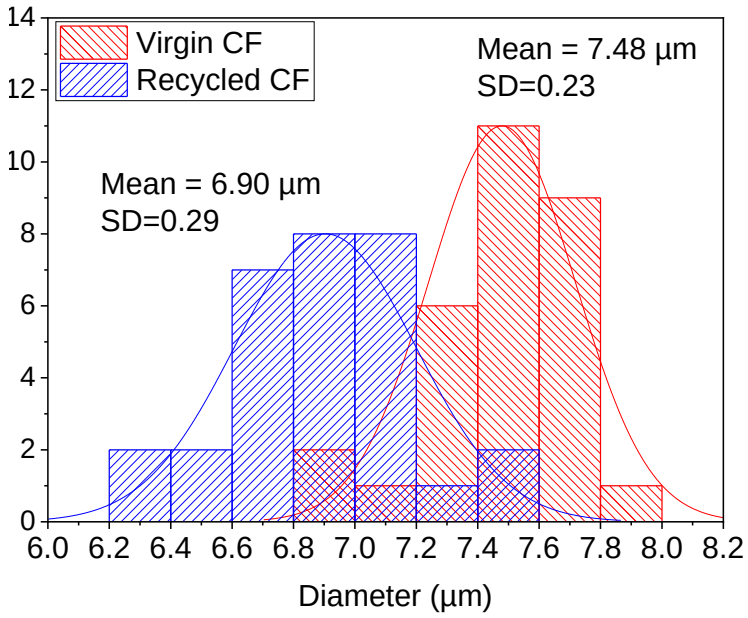

Figure 11 : vCF and rCF diameter measurements distribution

Further analysis was conducted on carbon fibre surface using SEM coupled to Energy Dispersive X-Ray (EDX) analysis in order to provide elemental identification and quantitative compositional information of virgin and recycled carbon fibre surfaces. Qualitative results, presented in Figure 12 showed clean virgin carbon fibre surface with only carbon chemical element on the surface. When residual spots on recycled CF was observed (Figure 12.b and Figure 12.c), the elemental composition was slightly different with the appearance of oxygen element, which accounts for around 3% in mass and some trace of sulphur (less than 0.4%). According to Chiang et al., carbon and oxygen were the most abundant elements at the PAN-based carbon fibre surface, with a considerable amount of nitrogen (Chiang et al., 2007). Therefore, the existence of oxygen atoms at recycled fibres surface could be linked to the decomposition of the polymer sizing layer from carbon fibre surface. In fact, before adding a specific sizing to protect fibre during textile processing and to provide a chemical link between the fibre surface and matrix, carbon fibre may exhibit an oxidative or non-oxidative surface treatment directly after carbonization step. In particular, carbon fibres used in this study are surface treated to enhance the adhesion properties with resin systems in a process known as oxidation, where oxygen atoms are chemically added to the surface of the fibre to increase the bonding characteristics.

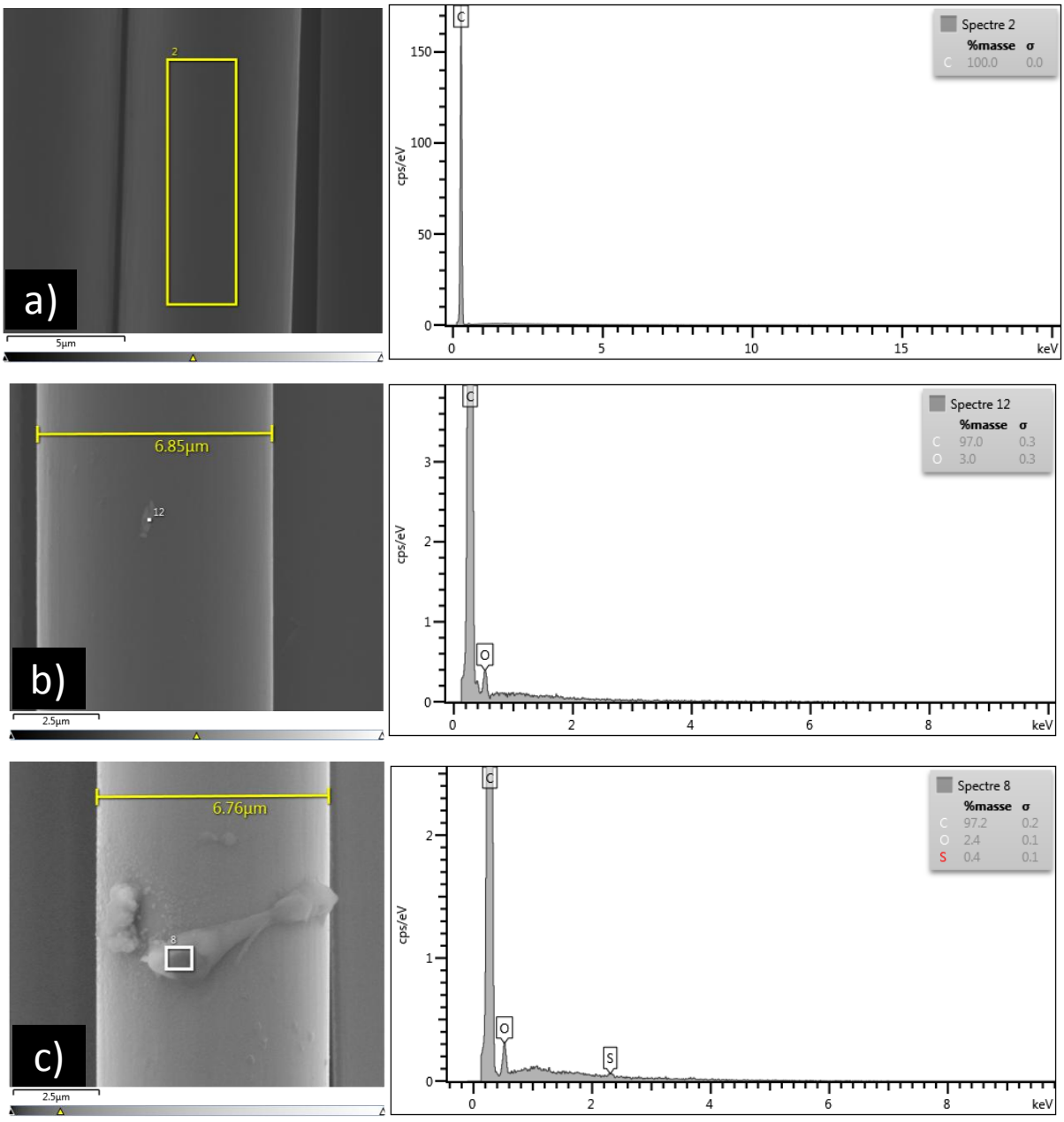

Figure 12 : SEM images with Energy Dispersive X-Ray (EDX) analysis on vCF surface (a) and residual impurities on rCF surfaces (b and c)

3.4. Analysis and results at composite scale

3.4.1. Tensile test

In order to assess mechanical properties and eventual effect of carbon fibre and matrix recovery and reuse, tensile tests were conducted at composite scale on both reference virgin material, semi recycled and fully recycled composites. As it was mentioned above, the limitation of reactor dimensions made it impossible to conduct tensile test on 250×25 mm² rCF/Elium samples as recommended by ISO 527-4 standard. A possible solution was to carry out tensile tests with smaller samples. Therefore, we proposed here samples with the half of nominal dimensions. In order to depict possible differences in

mechanical behaviour of scale different samples, tests were conducted in the longitudinal fibre direction on at least 5 samples until failure. Relative stress-strain curves are given by Figure 13.a and Figure 13.b.

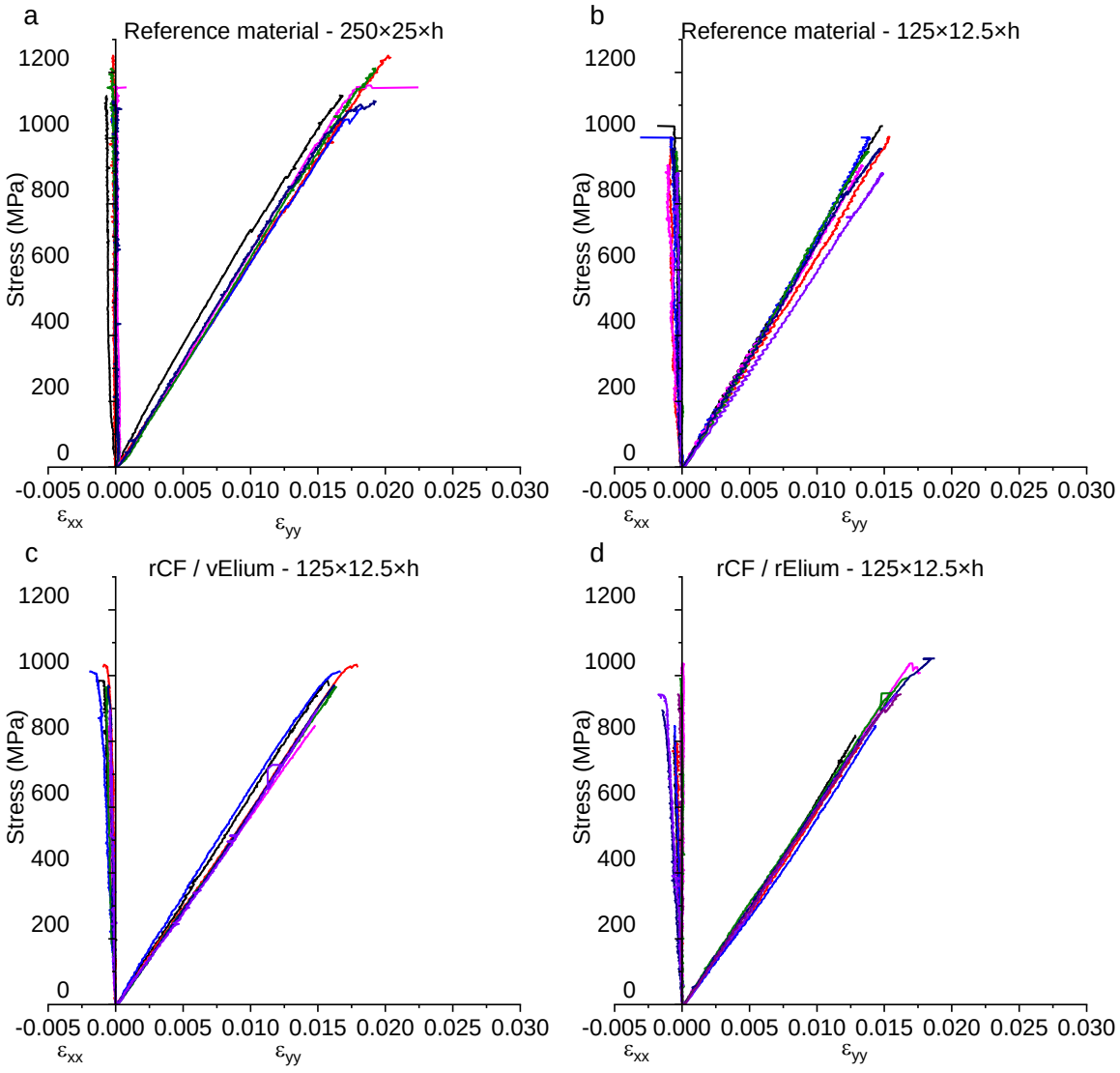

Figure 13: Uniaxial quasi-static tensile stress-strain curves of 0°/90° specimens of : (a) reference 250×25 samples, (b) reference 125×12.5 samples, (c) rCF/vElium and (d) rCF/rElium

In each graph, both longitudinal ε_{yy} and transverse ε_{xx} curves are presented from all tested specimens. Similar rigid and brittle behaviour can be described for both large and small samples in the longitudinal direction, where stress strain curves are linear until breaking. Furthermore, the use of a balanced CF biaxial fabric gives an explanation of the high transverse modulus compared to longitudinal one. However, a slight difference consisting of particularly a reduction of tensile strength and tensile strain at breaking can be spotted from Figure 13 and Figure 14. Young's modulus, evaluated in the strain interval of 0.05 – 0.25% using linear regression, decreased of around 5% from 65.3 GPa (Ref 1 for reference material with 250×25×h samples) to 62 GPa (Ref 1/2 for reference

material with 125×12.5×h samples), whilst tensile ultimate stress data revealed relatively more significant decrease of around 10% from reference value. This drop is related to weak edge fibre tows caused by machining step which causes premature failure and subsequently the debonding of aluminium tabs. The same trend was therefore also observed in the case of ultimate tensile strain between large and small samples. On the other hand, a similar Poisson's ratio was calculated for both sample geometries. Consequently, all differences in calculated properties between large and small composite samples were thus considered acceptable for further investigations in this work using small samples.

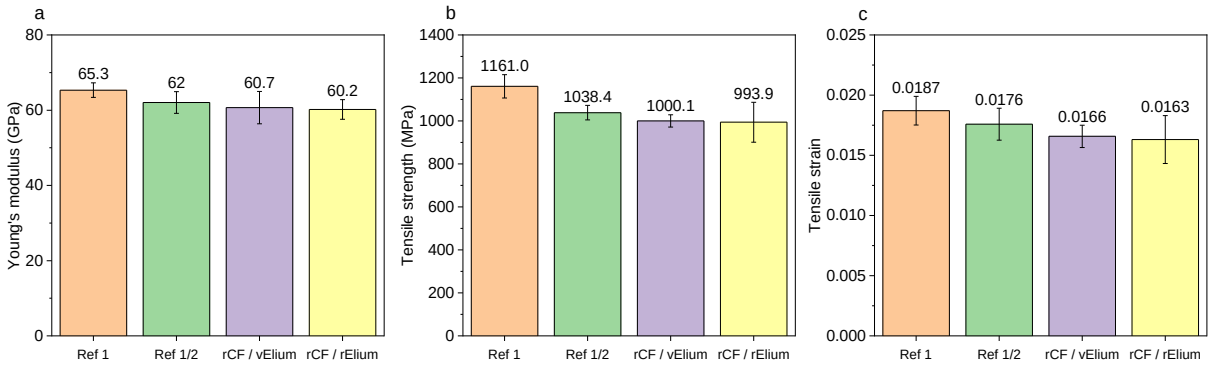

Figure 14 : Tensile Young modulus (a), ultimate tensile strength (b) and relative tensile strain at breaking (c) obtained by longitudinal tensile test on reference, semi-recycled and fully-recycled composites

As it is presented by stress-strain curves in Figure 13.c and Figure 13.d, the behaviour of semi-recycled (rCF/vElium) and fully recycled (rCF/rElium) is similar to that of the control material. An elastic and brittle behaviour is characterised by the linearity of the stress-strain curve until breaking. A set of at least 6 samples with aluminium tabs were tested for each case. The Young's modulus calculated for semi-recycled and fully recycled composites were 60.7 GPa and 60.2 GPa respectively, which represents 2.1% and 2.9% of decrease compared to initial reference composite. Regarding ultimate tensile stress and strain, the decrease was also statistically slight and within the standard deviation range (Figure 14). As load direction and fibre direction are superimposed in the case of axial tensile test, the results are known to be fibre-dependant. Therefore, an evidence can be obtained about the good quality of reclaimed CF by pyrolysis method under nitrogen atmosphere.

3.4.2. Interlaminar shear strength ILSS

In order to go further in the comparison of reference material compared to semi-recycled and full recycled composites, interlaminar shear strength test (also known as short beam test) was performed on a 5 mm thick (8 plies) composites. The span length of 21 mm was fixed with reference to sample thickness, which was found to be 5.15 mm and 5.26 mm for reference and recycled composites, respectively. Sample length and width were then 30 mm and 10 mm as recommended by the ASTM D2344 standard. The load-displacement curves of eight samples from each material are presented in

Figure 15. As it is known from test standard, the ILSS is commonly calculated from the first apparent discontinuity and drop in the load-displacement curve using Equation 5. The acceptance of the test is directly related to the failure mode, which has to be only interlaminar failure mechanisms. As we deal with highly heterogeneous materials, other failure modes could take place like tension and compression failure. Moreover, the failure modes strongly lie on fibre / matrix interface quality and bonding stiffness. It is clear from Figure 15.a that, for reference material, degradation mechanism other than interlaminar shear one have occurred as the drop of the load-displacement curve is not instantaneous. However, when measurement reproducibility is taken into account, an interlaminar shear strength value can be attributed to reference composite samples. Concerning rCF based composites, around all samples seems to exhibit an interlaminar failure. A single or multiple sharp step drop in load-displacement curve confirm the fact that interlaminar shear failure is occurring rather than tensile or compression failure (Bieniaś et al., 2020). In addition, we performed calculations to ensure that at this load, the shear strength did not exceed bending strength. Nevertheless, the ILSS results from reference material samples should be taken with caution. As it is for reference material curves, Figure 15.b and Figure 15.c show a good data reproducibility and many behaviour similarities. However, semi-recycled samples showed a clear drop in the curve after reaching a maximum load at 0.65 mm displacement, while full recycled samples showed a first slight drop at 0.5 mm followed by an increasing load until failure, which occurred at around 0.8 mm displacement. Another difference is maximum load level, which is significantly higher for rCF based composites compared to reference composite which leads to a subsequent higher interlaminar shear strength. This latter passed from 18.7 MPa to 28.4 MPa by substituting virgin fibre by recycled fibres, which represents around 35% increase. For full recycled composite, the increase rate is around 30% as presented in Figure 16. A plausible explanation of this behaviour difference is attributed to fibre/matrix compatibility. In fact, as mentioned before, the virgin carbon fibre used in this study does not have a specific sizing or surface treatment to application with acrylic matrix systems. This may conduct to a poor fibre/matrix bonding as most likely the sizing on carbon fibre is being partially dissolved in the acrylic resin during infusion and before complete polymerisation, as proposed by Hendlmeier et al. (Hendlmeier et al., 2019). In contrast, an interlaminar failure could indicate the presence of a good fibre/matrix interface bonding as found when rCF are used with either virgin or recycled matrix. Therefore, as the decomposition of fibre sizing using depolymerisation was highlighted by TGA and diameter measurements using SEM, one can suppose that Elium acrylic resin system is more likely to be compatible with desized carbon fibre. This issue must be understood before considering the finding for future work, particularly because of the possible influence of residual polymer on rCF surface to this enhanced bonding.

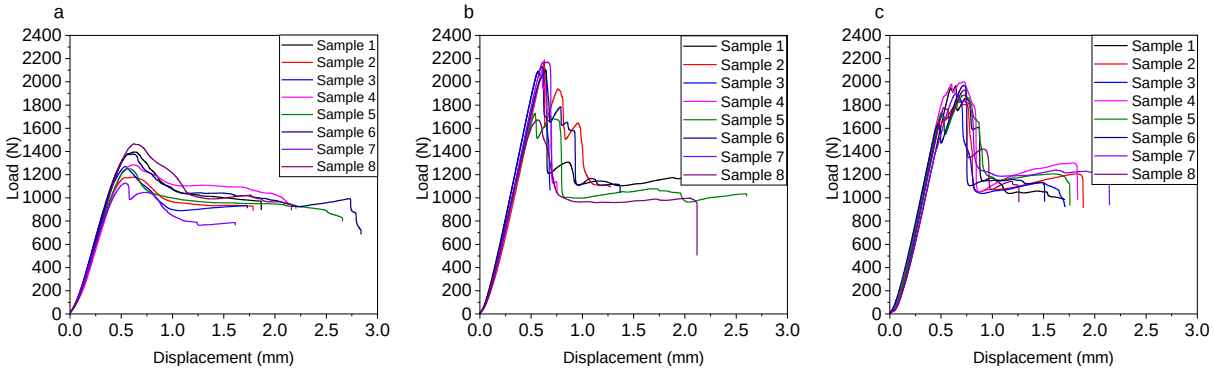

Figure 15 : ILSS load-displacement curves of (a) reference samples, (b) rCF/vElium samples and (c) rCF/rElium samples

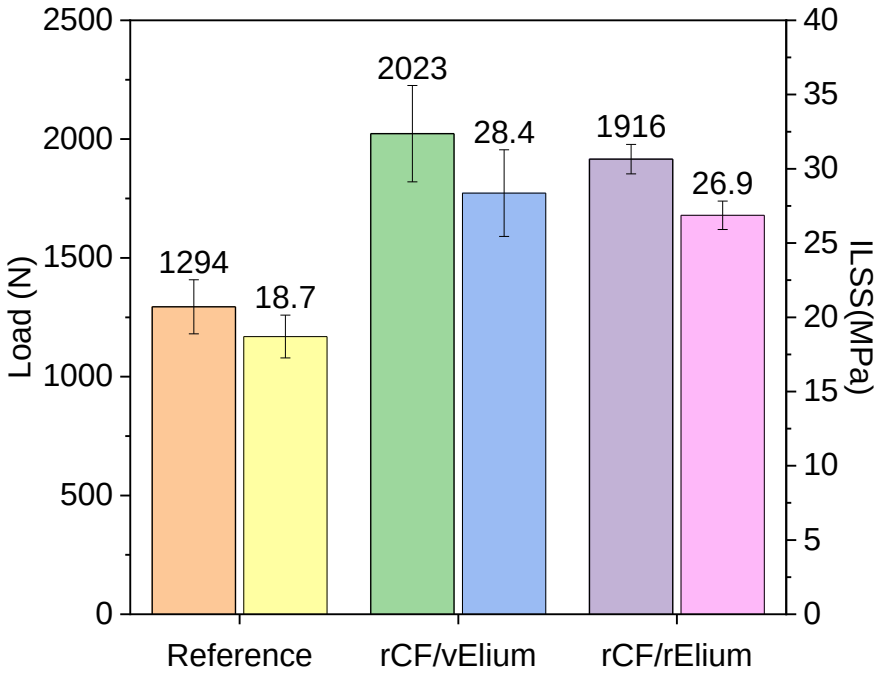

Figure 16 : Comparison of maximum load and calculated Interlaminar Shear Strength for reference, semi-recycled and full recycled composites

3.4.3. Dynamic Mechanical Analysis

In order to investigate the viscoelastic behaviour of the studied materials, DMA tests were conducted in dual cantilever setup for reference composite as well as rCF/vElium and rCF/rElium composites. The loss factor (tan δ) and storage elastic modulus (E') are reported in Figure 17.a and Figure 17.b. It is worth to note that at least three specimens were tested for reproducibility of the results. The glass transition temperature T_g was evaluated from loss factor (tan δ) peak. A significant difference of around 10 °C was found between reference material and rCF based composites. In addition, reference material was also found to have a higher damping peak and a 10 °C shift on tan δ peak onset. As the loss factor is defined by the ratio of loss modulus to storage modulus, a higher peak on the cure corresponds to higher molecular mobility by the effect of temperature. As the same virgin Elium resin

was employed for both reference and rCF/vElium composite, the difference may then come from different polymerisation conditions in the absence of polymer sizing on fibre surface or from enhanced fibre/matrix bonding as previously discussed. These differences in loss factor curves confirm previous results on the drop of ILSS of reference materials. In addition, the presence of fibre leads to constraints during the matrix relaxation step. As temperature increases, the free volume related with mobile chain segments increases (Raponi et al., 2018). The side chains and localised groups mobility causes a decrease of the storage modulus due to reduced resistance of the material to deformation (Figure 17.b). In the first part, the materials are in the glassy state and present a comparable initial storage modulus of around 21 GPa. A significant difference was then observed on storage modulus decrease onset temperature. Here also the reference composite sample presented more accentuated decrease in elasticity modulus caused by greater mobility of polymer chains. The similarities found in the rCF reinforced composites lead to a plausible hypothesis that recovered MMA monomer after depolymerisation process and further steps towards re-polymerisation did not affect the resin viscoelastic and mechanical properties. In order to confirm this hypothesis, DMA tests were performed on neat resin samples having 80×10×2 mm^3 dimensions and related results are presented in Figure 17.c and Figure 17.d. As it can be noticed, the loss factor curves present a clear peak of around 0.55 magnitude. A slight difference of around 3.5 °C can therefore be noticed between virgin and recycled neat Elium resins. On the other hand, nearly superimposed storage modulus curves were recorded with an initial value of around 2 GPa. All these findings lead to admit the hypothesis of the good properties of recovered Elium resin as no significant differences were found compared to virgin resin in addition to the good retention of mechanical properties with regards to composite samples.

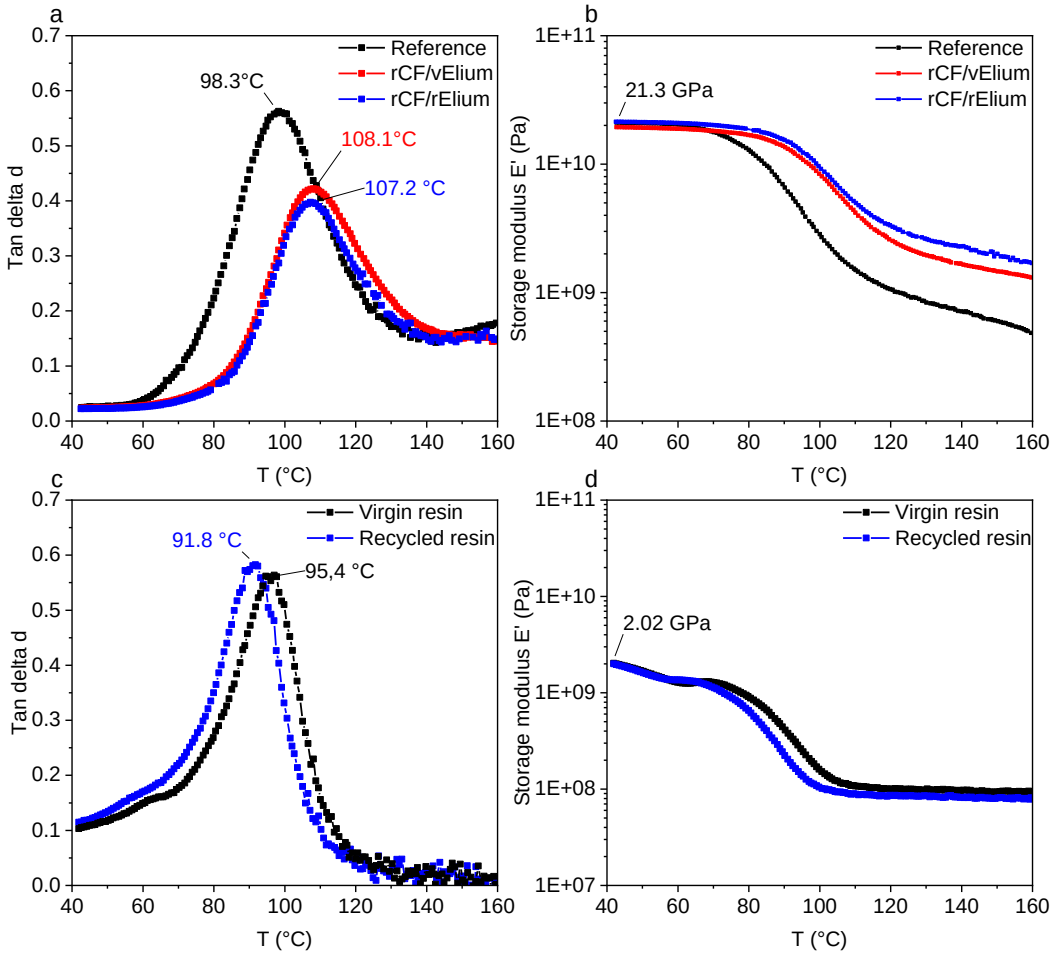

Figure 17 : DMA loss factor (a and c) and storage modulus (b and d) results as a function of temperature of different composites and resins samples

4. Conclusions

This study was conducted with the aim to establish a first proof of concept of the recyclability of a carbon fibre reinforced thermoplastic composite by pyrolysis method. The resin infused composite having a biaxial carbon fibre as reinforcement was depolymerised at a temperature range of 350 – 450 °C. The solid residue of the pyrolysis method containing carbon fibres accounted for around 72 %, whereas condensed gases fraction was about 26 %, from which a purified monomer solution was used to formulate the recycled Elium matrix. TGA on reclaimed fibres showed the degradation of sizing layer which thickness was found around 300 nm. Reclaimed carbon fibre with recycled matrix was used to remanufacture semi-recycled and fully-recycled good quality composites by resin infusion with around 55% fibre volume fraction. The mechanical properties were sufficiently retained after tensile modulus compared to reference material. The changes were less than 3% for the tensile modulus and 4% for tensile strength. The same trend was found by dynamic mechanical analysis, with some clear similarities between virgin and recycled Elium resin. Interlaminar shear analysis

highlighted a significantly enhanced interfacial strength compared to reference material and these findings were confirmed by DMA results.

This is the first time this approach is proposed for a full valorisation of reclaimed carbon fibre and Elium monomer from reference material using CF reinforced Elium composites through pyrolysis. The originality of this study was the use of the continuous and aligned carbon fibres with either virgin or recycled matrix, which showed promising mechanical behaviour that is from 2% to 3% less than reference material.

Acknowledgement

Authors would like to acknowledge the financial support from Occitanie region in France and REV inside, France as project partner.

References

Amaechi, C. V., Agbomerie, C.O., Sotayo, A., Wang, F., Hou, X., Ye, J., 2020. Recycling of Renewable Composite Materials in the Offshore Industry, in: Encyclopedia of Renewable and Sustainable Materials. Elsevier, pp. 583–613. https://doi.org/10.1016/B978-0-12-803581-8.11445-6

Bieniaś, J., Jakubczak, P., Drożdziel, M., Surowska, B., 2020. Interlaminar shear strength and failure analysis of aluminium-carbon laminates with a glass fiber interlayer after moisture absorption. Materials (Basel). 13, 1–14. https://doi.org/10.3390/ma13132999

Boulanghien, M., 2014. Formulations de composites thermoplastiques à partir de fibres de carbone recyclées par vapo-thermolyse. Ecole des Mines d'Albi- Carmaux.

Carbon fiber reclamation: Going commercial [WWW Document], n.d. URL https://www.compositesworld.com/articles/carbon-fiber-reclamation-going-commercial (accessed 8.4.20).

Chen, J., Wang, J., Ni, A., 2019. Recycling and reuse of composite materials for wind turbine blades: An overview. J. Reinf. Plast. Compos. 38, 567–577. https://doi.org/10.1177/0731684419833470

Chiang, Y.C., Lee, C.Y., Lee, H.C., 2007. Surface chemistry of polyacrylonitrile- and rayon-based activated carbon fibers after post-heat treatment. Mater. Chem. Phys. 101, 199–210. https://doi.org/10.1016/j.matchemphys.2006.03.007

Cousins, D.S., Lowe, C., Swan, D., Barsotti, R., Zhang, M., Gleich, K., Berry, D., Snowberg, D., Dorgan, J.R., 2017. Miscible blends of biobased poly(lactide) with poly(methyl methacrylate): Effects of chopped glass fiber incorporation. J. Appl. Polym. Sci. 134, 1–12. https://doi.org/10.1002/app.44868

Cousins, D.S., Suzuki, Y., Murray, R.E., Samaniuk, J.R., Stebner, A.P., 2019. Recycling glass fiber thermoplastic composites from wind turbine blades. J. Clean. Prod. 209, 1252–1263. https://doi.org/10.1016/j.jclepro.2018.10.286

Davies, P., Le Gac, P.-Y., Le Gall, M., 2017. Influence of Sea Water Aging on the Mechanical Behaviour of Acrylic Matrix Composites. Appl. Compos. Mater. 24, 97–111. https://doi.org/10.1007/s10443-016-9516-1

Dokos, L., 2013. Adoption of marine composites – a global perspective. Reinf. Plast. 57, 30–32. https://doi.org/10.1016/S0034-3617(13)70091-2

Eklund, B., 2013. Disposal of plastic end-of-life-boats. Copenhagen. https://doi.org/10.6027/TN2013-582

Feih, S., Mouritz, A.P., 2012. Tensile properties of carbon fibres and carbon fibre–polymer composites in fire. Compos. Part A Appl. Sci. Manuf. 43, 765–772. https://doi.org/10.1016/j.compositesa.2011.06.016

Ferriol, M., Gentilhomme, A., Cochez, M., Oget, N., Mieloszynski, J.L., 2003. Thermal degradation of poly(methyl methacrylate) (PMMA): Modelling of DTG and TG curves. Polym. Degrad. Stab. 79, 271–281. https://doi.org/10.1016/S0141-3910(02)00291-4

Godiya, C.B., Gabrielli, S., Materazzi, S., Pianesi, M.S., Stefanini, N., Marcantoni, E., 2019. Depolymerization of waste poly(methyl methacrylate) scraps and purification of depolymerized products. J. Environ. Manage. 231, 1012–1020. https://doi.org/10.1016/j.jenvman.2018.10.116

Hendlmeier, A., Marinovic, L.I., Al-Assafi, S., Stojcevski, F., Henderson, L.C., 2019. Sizing effects on the interfacial shear strength of a carbon fibre reinforced two-component thermoplastic polymer. Compos. Part A Appl. Sci. Manuf. 127, 105622. https://doi.org/10.1016/j.compositesa.2019.105622

ICOMIA, 2018. Recreational Boating Industry Statistics 2017.

Jayaram, S., Sivaprasad, K., Nandakumar, C.G., 2018. Recycling of FRP Boats. Int. J. Adv. Res. Eng. Technol. 9, 244–252.

Kaminsky, W., Franck, J., 1991. Monomer recovery by pyrolysis of poly(methyl methacrylate) (PMMA). J. Anal. Appl. Pyrolysis 19, 311–318. https://doi.org/10.1016/0165-2370(91)80052-A

Kim, K.-W., Lee, H.-M., An, J.-H., Chung, D.-C., An, K.-H., Kim, B.-J., 2017. Recycling and characterization of carbon fibers from carbon fiber reinforced epoxy matrix composites by a novel super-heated-steam method. J. Environ. Manage. 203, 872–879. https://doi.org/10.1016/j.jenvman.2017.05.015

Knight, C.C., Zeng, C., Zhang, C., Liang, R., 2015. Fabrication and properties of composites utilizing reclaimed woven carbon fiber by sub-critical and supercritical water recycling. Mater. Chem. Phys. 149, 317–323. https://doi.org/10.1016/j.matchemphys.2014.10.023

Mativenga, P.T., Shuaib, N.A., Howarth, J., Pestalozzi, F., Woidasky, J., 2016. High voltage fragmentation and mechanical recycling of glass fibre thermoset composite. CIRP Ann. - Manuf. Technol. 65, 45–48. https://doi.org/10.1016/j.cirp.2016.04.107

Monier, V., Hestin, M., Trarieux, M., Lemeillet, A., Laroche, M., Dupont, V., MAUMENEE, G., 2016. Etude préalable à la mise en place de la filière de collecte et de traitement des navires de plaisance et de sport hors d'usage sous la responsabilité des producteurs (REP).

Oliveux, G., Dandy, L.O., Leeke, G.A., 2015. Current status of recycling of fibre reinforced polymers: Review of technologies, reuse and resulting properties. Prog. Mater. Sci. 72, 61–99. https://doi.org/10.1016/j.pmatsci.2015.01.004

Önal, M., Neşer, G., 2018. End-of-life alternatives of glass reinforced polyester boat hulls compared by LCA. Adv. Compos. Lett. 27, 134–141. https://doi.org/10.1177/096369351802700402

Pickering, S.J., 2006. Recycling technologies for thermoset composite materials—current status. Compos. Part A Appl. Sci. Manuf. 37, 1206–1215. https://doi.org/10.1016/j.compositesa.2005.05.030

Pickering, S.J., Turner, T.A., Meng, F., Morris, C.N., Heil, J.P., Wong, K.H., Melendi, S., 2015. Developments in the fluidised bed process for fibre recovery from thermoset composites. CAMX 2015 - Compos. Adv. Mater. Expo.

Pimenta, S., Pinho, S.T., 2011. Recycling carbon fibre reinforced polymers for structural applications: Technology review and market outlook. Waste Manag. 31, 378–392. https://doi.org/10.1016/j.wasman.2010.09.019

Raponi, O. de A., Barbosa, L.C.M., de Souza, B.R., Ancelotti Junior, A.C., 2018. Study of the influence of initiator content in the polymerization reaction of a thermoplastic liquid resin for advanced composite manufacturing. Adv. Polym. Technol. 37, 3579–3587. https://doi.org/10.1002/adv.22142

Rybicka, J., Tiwari, A., Alvarez Del Campo, P., Howarth, J., 2015. Capturing composites manufacturing waste flows through process mapping. J. Clean. Prod. 91, 251–261. https://doi.org/10.1016/j.jclepro.2014.12.033

Sauer, M., 2019. Composites Market Report 2019 : The global CF - und CC-Market 2019 - Market developments, Trends, outlook and challenges.

Singh, M.M., Summerscales, J., Wittamore, K., 2010. Disposal of composite boats and other marine composites, in: Management, Recycling and Reuse of Waste Composites. Elsevier, pp. 495–519. https://doi.org/10.1533/9781845697662.5.495

Verma, S., Balasubramaniam, B., Gupta, R.K., 2018. Recycling, reclamation and re-manufacturing of carbon fibres. Curr. Opin. Green Sustain. Chem. 13, 86–90. https://doi.org/10.1016/j.cogsc.2018.05.011

Witik, R.A., Teuscher, R., Michaud, V., Ludwig, C., Månson, J.A.E., 2013. Carbon fibre reinforced

composite waste: An environmental assessment of recycling, energy recovery and landfilling. Compos. Part A Appl. Sci. Manuf. 49, 89–99. https://doi.org/10.1016/j.compositesa.2013.02.009

Witten, E., Mathes, V., 2019. The Market for Glass Fibre Reinforced Plastics (GRP) in 2019.

Ye, S.Y., 2012. Valorisation de déchets composites à renfort de fibres de carbone par un procédé de vapo-thermolyse. Université de Toulouse.

Zhang, J., Chevali, V.S., Wang, H., Wang, C.-H., 2020. Current status of carbon fibre and carbon fibre composites recycling. Compos. Part B Eng. 193, 108053. https://doi.org/10.1016/j.compositesb.2020.108053